ACS APPLIED MATERIALS & INTERFACES

Research Article

www.acsami.org

Copper Removal Using Electrosterically Stabilized Nanocrystalline Cellulose

Amir Sheikhi,[†,‡,§,∥] Salman Safari,[§,⊥,∥] Han Yang,[†,‡,§] and Theo G. M. van de Ven*[,†,‡,§]

[†]Department of Chemistry, [‡]Pulp and Paper Research Centre, Department of Chemistry, [§]Centre for Self-Assembled Chemical Structures, and [⊥]Department of Chemical Engineering, McGill University, Montreal, Quebec H3A 2A7, Canada

Supporting Information

ABSTRACT: Removal of heavy metal ions such as copper using an efficient and low-cost method with low ecological footprint is a critical process in wastewater treatment, which can be achieved in a liquid phase using nanoadsorbents such as inorganic nanoparticles. Recently, attention has turned toward developing sustainable and environmentally friendly nanoadsorbents to remove heavy metal ions from aqueous media. Electrosterically stabilized nanocrystalline cellulose (ENCC), which can be prepared from wood fibers through periodate/chlorite oxidation, has been shown to have a high charge content and colloidal stability. Here, we show that ENCC scavenges copper ions by different mechanisms depending on the ion concentration. When the Cu(II) concentration is low ($C_0 \lesssim 200$ ppm), agglomerates of starlike ENCC particles appear, which are broken into individual starlike entities by shear and Brownian motion, as evidenced by photometric dispersion analysis, dynamic light scattering, and transmission electron microscopy. On the other hand, at higher copper concentrations, the aggregate morphology changes from starlike to raftlike, which is probably due to the collapse of protruding dicarboxylic cellulose (DCC) chains and ENCC charge neutralization by copper adsorption. Such raftlike structures result from head-to-head and lateral aggregation of neutralized ENCCs as confirmed by transmission electron microscopy. As opposed to starlike aggregates, the raftlike structures grow gradually and are prone to sedimentation at copper concentrations $C_0 \gtrsim 500$ ppm, which eliminates a costly separation step in wastewater treatment processes. Moreover, a copper removal capacity of ~185 mg g^{-1} was achieved thanks to the highly charged DCC polyanions protruding from ENCC. These properties along with the biorenewability make ENCC a promising candidate for wastewater treatment, in which fast, facile, and low-cost removal of heavy metal ions is desired most.

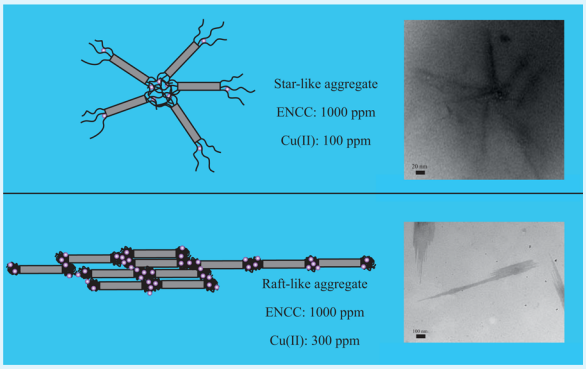

KEYWORDS: *sustainable adsorbent, nanocrystalline cellulose, copper removal, wastewater treatment, bridging aggregation*

INTRODUCTION

The presence of heavy metal ions such as copper in water can contaminate the food chain and have lethal effects on vital organs of not only humans but also all forms of life. Efficient removal of these pollutants is a prerequisite for wastewater recycling. Conventionally, heavy metal ion removal has been achieved using activated carbon in a liquid-phase adsorption process.[1] Due to the high cost of activated carbon, the search for other low-cost adsorbents has been at the center of many research studies on wastewater treatment. Typical examples are fly ash,[2] nanosized metal oxides,[3] silica gel,[4] zeolite,[5] lignin,[6] seaweed,[7] wool,[8] agricultural wastes such as coconut shell and rice husk,[9,10] chitin, and chitosan.[11]

Nanoadsorbents are of particular interest for large-scale water remediation, due to their high surface area, which, on the one hand, can increase the contact area between the adsorbent and the heavy metal ions[12,13] and, on the other, can be a substrate for the deposition of polyelectrolytes with high heavy metal ion removal capacity, thus assisting in their removal.[14−18] Moreover, upon adsorption of these polymers the colloidal stability of the hosting nanoparticles is increased, mainly due to the electrosteric effect of the adsorbed polymers.[19]

Recently, it has been shown that derivatives of cellulose, a ubiquitous and abundant product of nature, can be exploited for the purpose of heavy metal ion removal.[20−22] The most desirable cellulose derivatives for wastewater treatment are cellulose nanofibers including bacterial cellulose,[23] nanocrystalline cellulose,[24,25] and micro/nanofibrillar cellulose,[26,27] mainly because of their high surface area and feasibility of introducing functional groups with high affinity for heavy metal ions. Also, biodegradability and low cyto/genotoxicity of cellulose nanoparticles distinguish them from their inorganic counterparts.[28,29] Electrosterically stabilized nanocrystalline cellulose (ENCC) has been introduced recently by Yang et al. as a new derivative of cellulose,[30] in which dicarboxylated cellulose (DCC) chains are hypothesized to be protruding from the crystalline part. These

Received: February 19, 2015
Accepted: May 7, 2015
Published: May 7, 2015

DOI: 10.1021/acsami.5b01619
ACS Appl. Mater. Interfaces 2015, 7, 11301−11308

polyelectrolytes are highly charged, which impart ENCC with a charge content about 20 times higher than that of conventional NCC and result in a high stability even at salt concentrations as high as 200 mmol L^{-1}.[31] A schematic diagram of an ENCC particle is presented in Figure 1. Note that the size of ENCC

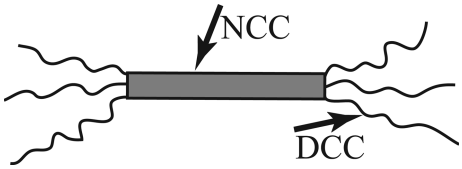

Figure 1. Schematic representation (not to scale) of an ENCC particle with its protruding dicarboxylated cellulose (DCC) chains.

crystalline part is similar to that of conventional NCC (ENCC length and width are 100−200 nm and ∼5−10 nm, respectively).

In this work, we investigate the mechanism of copper ion adsorption on ENCC at various Cu^{2+} concentrations using photometric dispersion analysis (PDA), dynamic light scattering (DLS), and transmission electron microscopy (TEM). Then the effect of Cu^{2+} initial concentration on ENCC copper removal capacity is studied.

MATERIALS AND METHODS

Materials. Q-90 bleached softwood pulp sheets (Domtar, Canada) were used as starting cellulose material. Copper(II) sulfate (anhydrous powder, ≥99.99%), NaCl (ACS reagent, ≥99%), NaOH (ACS reagent, ≥97%), sodium chlorite (80%), and sodium (meta)periodate (≥99.99%) were purchased from Sigma-Aldrich, Canada, and used without further purification. Nitric acid (ACS reagent, 68−70%) was purchased from ACP Chemicals Inc., Canada. Anhydrous ethanol (95.27%) was supplied by Fisher Scientific, Canada.

Methods. ENCC was produced according to the procedure outlined by Yang et al.[32] Briefly, softwood pulp was first oxidized by periodate for 96 h (1 g of pulp and 1.33 g of $NaIO_4$ were mixed with 66 mL of water in a beaker, which was wrapped with aluminum foil to prevent entry of any light), followed by overnight oxidation using sodium chlorite at pH = 5 (1.41 g of $NaClO_2$, 1.41 g of H_2O_2, 2.93 g of NaCl, and 50 mL of water were used for 1 g of periodate oxidized pulp). ENCC was separated from the two-step oxidized pulp suspension by the addition of ethanol followed by centrifugation.

Conductometric titration was performed to obtain the ENCC charge density using a Metrohm 836 Titrando titrator (Ontario, Canada). A sample with 0.02 g of solids and 2 mL of 20 mmol L^{-1} NaCl was added to 140 mL of Milli-Q water.[30] Starting from pH = 2.7, 10 mmol L^{-1} NaOH solution was added at 0.1 mL min^{-1} to the suspension up to pH = 11. This furnished the equivalent base volume required to neutralize the surface active groups from which the carboxyl content was calculated to be 5.5 ± 0.25 mmol g^{-1}.

Aggregation of ENCC in copper solutions was studied using a photometric dispersion analyzer (PDA2000, Rank Brothers Ltd., U.K.), in which flocculation causes an increase in the root mean square (RMS) value of the alternating current (ac) signal (proportional to the transmitted light intensity fluctuations), while the direct current (dc) component of the signal (proportional to the average transmitted light intensity) remains constant as long as the suspension turbidity does not change significantly. PDA is a powerful technique to monitor aggregate stability at various shear rates in real time.[33] An adequate amount of ENCC was added to a 8 mL copper solution at a desired concentration, which was being constantly pumped using a peristaltic pump at a constant flow rate corresponding to an average shear rate $\dot{\gamma} \approx 390\ s^{-1}$. The ENCC concentration after addition was 1000 ppm.

Transmission electron microscopy (TEM) specimens were prepared by leaving 10 μL of the Cu(II)/ENCC supernatant on a carbon-coated square mesh copper grid (mesh size 400, Electron Microscopy Sciences, USA) for 30 s. The liquid was absorbed from the side with a laboratory tissue, followed by air drying at room temperature for 5 min and imaging using Tecnai 12, 120 kV, Field Emission Inc.

The particle size distribution was obtained using dynamic light scattering at a 90° scattering angle and room temperature (Brookhaven light scattering instrument coupled with a BI9000 AT digital correlator).

A stock aqueous solution of 1000 ppm of copper was prepared by dissolving copper sulfate in distilled water, which was diluted to the desired copper solutions by adding distilled water. To perform adsorption experiments, 200 μL of a 20000 ppm ENCC suspension was added to 4 mL of a copper solution with an initial concentration, C_0, ranging from 300 to 900 ppm. For each treated sample, a control copper solution was prepared against which ENCC removal and capacity were compared. All Cu(II)−ENCC dispersions adjusted themselves to pH = 4 ± 0.2, which is well below the copper hydroxide precipitation pH.[34] The Cu(II)−ENCC dispersions were filtered with 100 nm nylon syringe filters (Membrane-Solutions, China), and the filtrate was examined with DLS to evaluate the particle separation efficiency, followed by nitric acid digestion of the supernatant (final acid concentration 1 mol L^{-1}). The copper concentrations of treated and control samples were obtained using inductively coupled plasma emission spectroscopy (ICP-ES, Thermo Scientific 6000 series), which was calibrated using standard copper solutions (reference standard copper solution (1000 ppm ± 1%), Fisher Scientific, Canada).

RESULTS AND DISCUSSION

Despite the high colloidal stability of ENCC in the presence of monovalent ions,[31] addition of multivalent cations, such as Cu(II), to ENCC suspension may result in an instantaneous increase in particle size and aggregation. Figure 2 shows the ratio of the RMS (flocculation index, FI)[35] to dc signal, obtained by PDA, as an indication of aggregate size and number density versus time. Changes in the dc signal are mainly caused by the turbidity variation of the sample and approximately 2 orders of magnitude smaller than the ac fluctuations. The flocculation index of the initial copper solution C_0 is zero, because the solution is completely transparent. When the ENCC is added to the copper solution of concentration $C_0 \approx 100$ or 200 ppm, no change in the ratio is observed, probably due to the formation of aggregates smaller than the PDA detection limit or no aggregation occuring and light scattering by ENCC is low. On the other hand, for a copper solution with $C_0 \approx 300$ ppm, the FI starts growing with time and reaches a plateau after ∼12 min (Figure 2a), which suggests that aggregation has reached a steady state (i.e., a dynamic equilibrium between formation and breakup). The applied shear rate was $\dot{\gamma} \approx 390\ s^{-1}$ in a tube with inner diameter ≈ 3.2 mm. Increasing the average shear rate above 390 s^{-1} results in bubble formation in the circulating dispersion, which complicates the interpretation of aggregate stability. At higher copper concentrations, i.e., 400 and 500 ppm, the flocculation index reaches the instrument detection limit (ratio = 10) in ∼15 and 10 min after copper addition, respectively. These results show that in the case of a uniform initial copper concentration, at high enough final ENCC concentration (1000 ppm), stable copper-mediated ENCC aggregates are formed in a time scale of a few minutes.

To shed light on how the local copper concentration affects the aggregate formation and to better understand the effect of copper and ENCC interactions, PDA experiments were also conducted on the aggregation of ENCC dispersions (1000 ppm) with stepwise addition of a concentrated copper solution (∼20 000 ppm) at the same average shear rate of 390 s^{-1} to achieve C_0 spanning from 100 to 500 ppm (Figure 2b). Similar to a copper solution, an ENCC suspension yields $FI = 0$; however, upon copper addition, a sudden increase in the ratio occurs.

DOI: 10.1021/acsami.5b01619
ACS Appl. Mater. Interfaces 2015, 7, 11301−11308

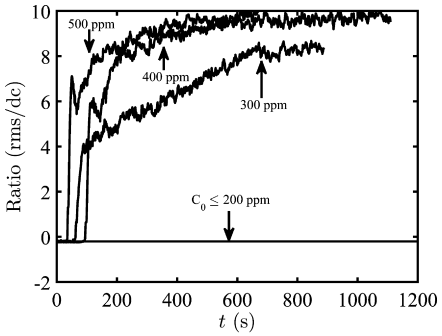

(a) ENCC is added to the copper solution.

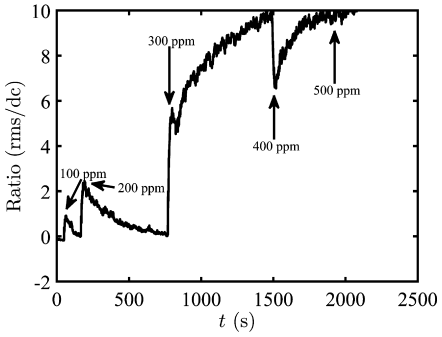

(b) Copper solution is added to the ENCC dispersion.

Figure 2. (a) Flocculation dynamics of ENCC (concentration C_{ENCC} = 1000 ppm) upon addition to copper solutions with $C_0 \lesssim 200$ ppm, $C_0 \approx$ 300, 400, and 500 ppm, determined by photometric dispersion analysis (PDA), expressed in terms of ratio (rms/dc) versus time (t). (b) Flocculation dynamics of ENCC dispersion (1000 ppm) upon addition of 20 000 ppm copper solution to achieve the desired copper concentration (shown with arrows) using PDA. At $C_0 \lesssim 200$ ppm, high local copper concentration results in detectable ENCC aggregates, which are unstable against the shear; however, at $C_0 \approx 300$ ppm, the increase of ratio suggests a shear-induced aggregation. At $C_0 \gtrsim 300$ ppm, the aggregates remain stable. Stable aggregate formation is of great importance in particle separation processes after ion adsorption.

When $C_0 \approx 100$ or 200 ppm, the FI relaxes back to zero after a few minutes, indicating that the final ENCC aggregates have become smaller than the detection limit of the instrument. Note that at $C_0 \lesssim 200$ ppm and ENCC concentration of 1000 ppm, when ENCC is added to Cu(II) solution, the initial copper concentration remains uniform and the FI adopts a zero value. Increasing the copper concentration to 300 ppm increases the FI in a fashion similar to the one seen in Figure 2a. Raising copper concentration more increases the ratio further, reaching the instrument detection limit at $C_0 \gtrsim 400$ ppm.

TEM images of ENCC aggregates reveal different morphologies at different copper concentrations. While individual ENCC particles are rodlike (Figure 3a), aggregates of ENCC particles at copper concentration $C_0 \approx 100$ ppm are starlike consisting of a few ENCCs aggregated from one end (Figure 3b). On the other hand, at copper concentration $C_0 \approx 300$ ppm lateral and head-to-head aggregation of ENCCs are observed, which results in raftlike features (Figure 3c).

Our hypothesis is that at copper concentrations C_0 <300 ppm, while some ENCC particles are (nearly) completely neutralized by copper ions, others are partially saturated. When these particles come into contact, they form aggregates, which results in ion redistribution in the overlapping protruding chains. This ion distribution weakens the bonds, leading to a transient agglomeration of ENCC particles. The breakup of these transient aggregates leads to the starlike entities at the final steady state condition (Figure 4a). The initial agglomeration of ENCCs is transient and only occurs when concentrated copper is added to ENCC suspension, perhaps due to the high local Cu/ENCC ratio resulting in agglomerates, which are broken into individual starlike features in a few minutes by the shear. In the absence of shear, we observed that these agglomerates sediment and do not break within the course of several days. Note that since the starlike entities are still charged and stable, similar to individual ENCC particles, the drying effect is probably minimal. The shaded area around the features may indicate that the initial droplet was broken into several small droplets upon drying (drying artifact).

At higher copper concentrations, 300 or 400 ppm, ENCC aggregates grow gradually with time regardless of the way ENCC and copper are mixed, since the copper concentration is sufficiently high to neutralize ENCC particles. Noteworthy is that lowering the pH facilitates the breakup of raftlike aggregates by replacing some of the adsorbed copper ions with protons. Previously, we showed that protonated ENCC particles do not aggregate even at pH = 1.5,[31] attesting to the importance of steric effects in stabilizing ENCC particles.

This explanation is corroborated further by the DLS size distribution of ENCC aggregates. At neutral condition, ENCC particles are monodisperse with effective diameter $d \approx 185$ nm (Figure 5). Increasing the copper concentration (e.g., 100 ppm, shown with circles) has a dual effect: while the size of some particles decreases due to the contraction of protruding polymer chains because of the decrease in pH,[31] likely because of formation of $Cu(OH)^+$, others experience a size increase due to the formation of stable polydisperse aggregates. On the other hand, a higher copper concentration, $C_0 \gtrsim 300$ ppm, results in almost complete neutralization of ENCC by copper ions. Neutralized particles tend to aggregate head-to-head and laterally (Figure 3c). These raftlike features grow further over a time period of a few minutes mainly due to shear-induced collisions (Figure 4b). DLS results are in good agreement with the PDA and TEM observations. Increasing the Cu(II) concentrations $C_0 \gtrsim 300$ ppm increases the aggregates size, which are sufficiently large at $C_0 \geq 500$ ppm that no particle is detected in the supernatant, implying that all ENCC aggregates sediment. This is mainly due to the large raftlike ENCC flocs that have been completely neutralized by copper ions (Figure 3c), which can settle even in the absence of a centrifugal force (Figure S1, Supporting Information). When $300 \lesssim C_0 \lesssim 500$ ppm, DLS results indicate that raftlike aggregates collide and grow slowly over the course of 2 days, due to the Brownian motion (Figure S2, Supporting Information). Moreover, at copper concentrations $300 \lesssim C_0 \lesssim 500$ ppm, filtration with 100 nm syringe filters removed all particles from the Cu(II) solution, whereas at $C_0 \lesssim$ 300 ppm, filtration removed only some of the aggregates. Perhaps, in the latter case, the applied shear force in the syringe filter nanopores is strong enough to break the aggregates into individual ENCCs, which can pass through the filter.

Explaining the aggregation mechanisms of ENCCs quantitatively is more complicated. The difficulty arises when one wants to calculate aggregation and breakup rate coefficients. Both of these coefficients depend on the number of particles, their diameters, and the collision rate.[33,36] As seen in Figure 5, ENCC aggregates are highly polydisperse, which can be attributed to the broad size distribution of freely suspending raftlike ENCC aggregates. Moreover, dicarboxylated cellulose (DCC) chains are protruding from the rodlike crystalline part of ENCC, which complicates calculation of the collision rate coefficient.

DOI: 10.1021/acsami.5b01619
ACS Appl. Mater. Interfaces 2015, 7, 11301−11308

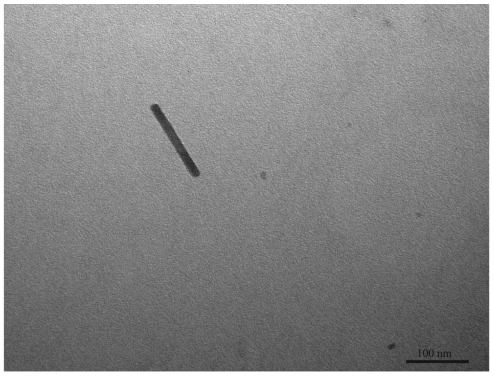

(a) ENCC

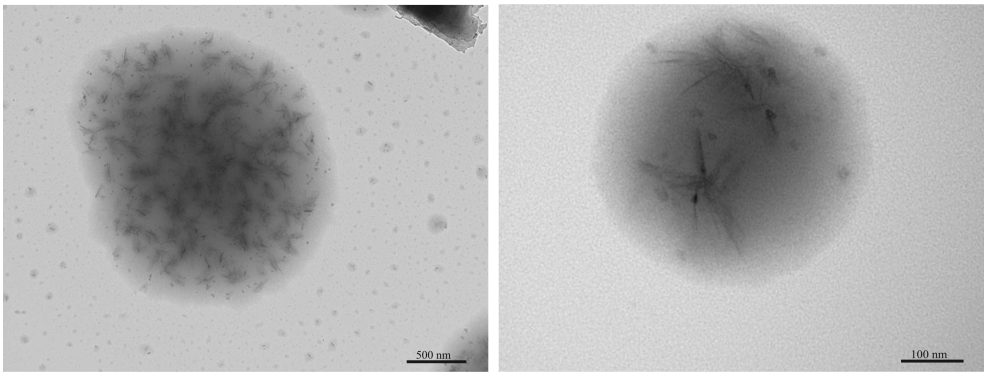

(b) $C_0 \approx 100$ ppm

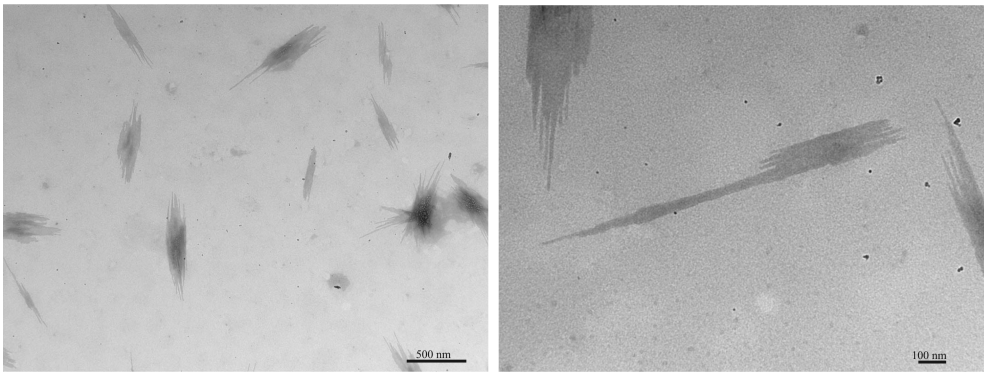

(c) $C_0 \approx 300$ ppm, supernatant

Figure 3. Transmission electron microscopy (TEM) images of an individual ENCC (a), starlike ENCC aggregates in the presence of 100 ppm of copper (b), and raftlike ENCC aggregates in a 300 ppm of copper solution (c).

As suggested by the flocculation dynamics, efficient Cu(II) ion separation condition is at $C_{ENCC} = 1000$ ppm and $C_0 \gtrsim 300$ ppm. Accordingly, we performed adsorption experiments by varying C_0 between 200 and 900 ppm. The copper removal versus initial copper concentration is presented in Figure 6. The maximum removal $R_{max} \approx 63\%$ at pH ≈ 4 is achieved at $C_0 \approx 300$ ppm, because at lower Cu(II) concentrations, a complete adsorbent separation cannot be achieved either by filtration or by centrifugation, due to the weak particle bridging. Note that using filters with diameter less than 100 nm is not feasible due to the extremely high pressure drop across the membrane. The decreasing trend of removal versus initial copper concentration suggests that the maximum Cu(II) removal capacity of ENCC has been achieved. To evaluate this, the equilibrium copper removal capacity, q_e (mg g^{-1}), in the samples with final volume V (m^{-3}), $q_e = (C_0 - C_e)V/m_{ENCC}$, is plotted versus the ratio of equilibrium copper concentration over the amount of ENCC in Figure 7, in which C_0 (ppm) is the initial copper concentration, C_e (ppm) is the equilibrium copper concentration in the solution, and m_{ENCC} (g) is the ENCC dosage. The possible complexations of copper with carboxyl groups can be summarized in the following reactions[37]

$$COO^- + Cu^{2+} \rightleftharpoons [Cu(COO)]^+$$

$$COO^- + [Cu(COO)]^+ \rightleftharpoons Cu(COO)_2$$

$$COO^- + [Cu(OH)]^+ \rightleftharpoons Cu(COO)(OH)$$

$$COO^- + H^+ \rightleftharpoons COOH$$

DOI: 10.1021/acsami.5b01619
ACS Appl. Mater. Interfaces 2015, 7, 11301−11308

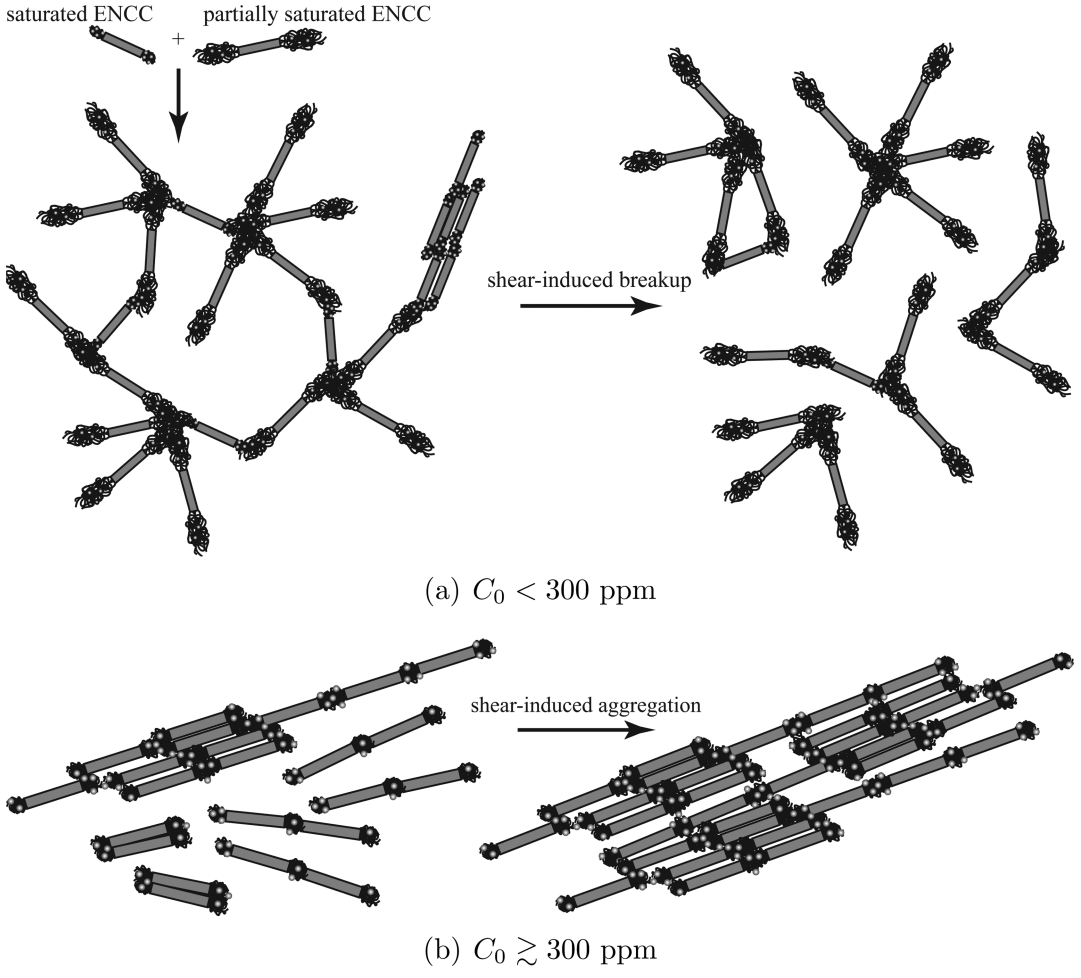

Figure 4. (a) Hypothesized mechanism of aggregation and breakup of ENCCs at copper concentration $C_0 < 300$ ppm. (b) Hypothesized mechanism of ENCC aggregation at copper concentration $C_0 \gtrsim 300$ ppm.

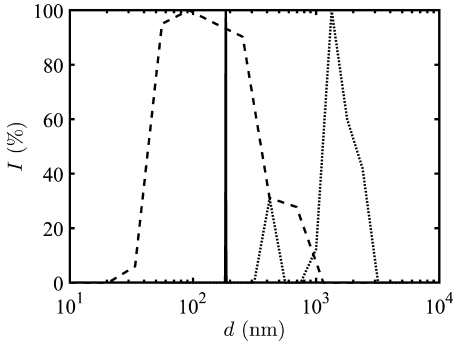

Figure 5. ENCC (1000 ppm) size distribution after 17 h unperturbed residence in copper solutions $C_0 = 0$ (solid line, which has a narrow size distribution), 100 (dashed line), and 400 ppm (dotted line), obtained by dynamic light scattering (DLS). Note that all samples are collected from the PDA experiments. At $C_0 \gtrsim 500$ ppm, DLS was not able to detect any particle in the supernatant.

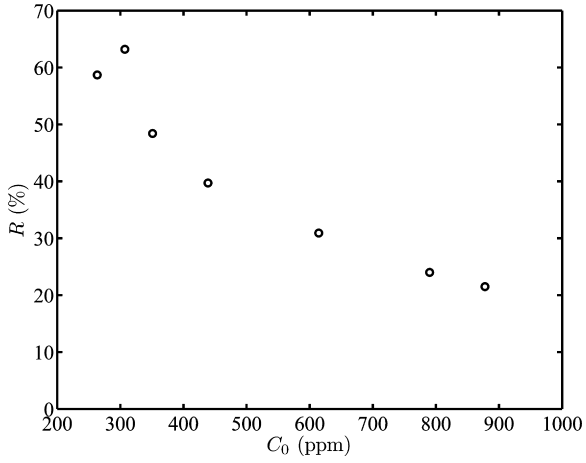

Figure 6. Copper removal $R = (C_0 - C_e)/C_0$ versus initial copper concentration C_0. The equilibrium copper concentration C_e is obtained from ICP experiments with less than 2% error. Note that R at $C_0 \lesssim 250$ ppm is an underestimation of the ENCC performance, because of failed tries to separate small ($d < 100$ nm) ENCCs.

Quantitative analysis of these complexes is cumbersome since their formation constants on ENCC's protruding polymers cannot be merely borrowed from the ones measured in the literature for carboxylic acid by conductometry; however, since all of ENCC aggregates precipitate, $Cu(COO)_2$ or Cu(COO)-(OH) can be considered as the dominant species. Interestingly, the experimentally determined equilibrium removal capacity, 185 ± 4 mg g^{-1}, is close to the stoichiometric capacity of ENCC, i.e., 2.75 ± 0.125 mmol or 175 ± 8 mg Cu(II) per 1 g of ENCC, the difference not being significant. Note that the excess copper concentration may be the reason for achieving the maximum Cu(II) removal capacity of ENCC at pH 4, for which in the absence of excess copper about one-half of the carboxyl groups

DOI: 10.1021/acsami.5b01619
ACS Appl. Mater. Interfaces 2015, 7, 11301−11308

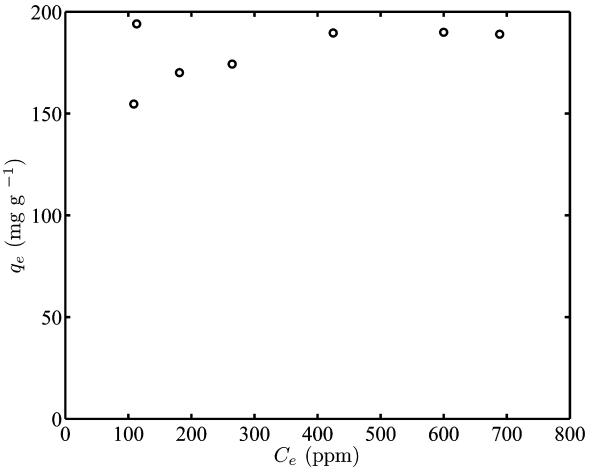

Figure 7. Copper removal capacity of ENCC $q_e = (C_0 - C_e)V/m_{ENCC}$ versus equilibrium copper concentration C_e. Sample volume $V \approx 4$ mL.

are protonated. Adding excess Cu(II) shifts the first three equilibria shown above to the right and the last one to the left. The removal capacity of ENCC is compared to some other adsorbents available in the literature (Table 1).

Table 1. Cu(II) Removal Performance of ENCC as Compared to Some Available Adsorbents

adsorbent	q_e (mg g^{-1})	pH	ref
ENCC	185	4 ± 0.2	this work
amino-modified nanostructured microfibrillated cellulose	174	5	26
carboxymethylated-bacterial cellulose	9.7	4.5	23
polymer-modified magnetic nanoparticles	129	5.5	17
anisotropic layered double hydroxide nanocrystal @ carbon nanosphere	20	5.7	15
carboxylated alginic acid	159	4	38
oxidized cellulose powder (sodiumm metaperiodate)	236	4.6	39
chitosan (various forms[a])	20−325	4.5−6	40
chitosan-coated perlite beads	196.08	5	41
chitosan coated perlite beads	104	4.5	40
tea waste	48	5.5 ± 0.5	42
tobacco dust	36	6.5−7.2	43
tartaric acid-modified rice husk	31.85	4	44
newspaper pulp	30	5.5	45
sugar beet pulp	28.5	4	46
chitosan-cellulose blend	26.7	5.8	47
banana pitch	13.46	4.5	48
wheat shell	10.84	5	49
NaOH-treated poplar sawdust	6.92	4	50
chitosan-cellulose hydrogel beads	5 or 14.5[b]	5	51
activated carbon (coal)	4.4	5	52
chitosan-coated cotton fibers	1.0	4	53

[a]The chitosan extracted from shrimp has a high removal capacity q_e = 300 mg g^{-1}. [b]Non-cross-linked hydrogels provide greater q_e.

CONCLUDING REMARKS

In this work, we explored the possibility of using electrosterically stabilized nanocrystalline cellulose (ENCC) as a biorenewable nanoadsorbent for copper removal from water. Photometric dispersion analysis was used to study the flocculation dynamics of ENCC aggregates in the presence of copper ions at a constant shear rate. It was found that at up to a copper/ENCC ratio of ~200 mg g^{-1} the aggregates were sufficiently small and stable which caused no change in the PDA flocculation index; however, at higher ratios, the aggregates started to grow gradually until they leveled off at a high flocculation index or reached the instrument detection limit. TEM images of suspended aggregates at a copper/ENCC ratio ≈ 100 mg g^{-1} revealed the presence of starlike features consisting of a few ENCC particles aggregated from one end, whereas at a copper/ENCC ratio ≈ 300 mg g^{-1}, lateral and head-to-head aggregation of ENCCs led to raftlike aggregates, perhaps because of charge neutralization, which sediment shortly after formation, eliminating a costly separation step in wastewater treatment. Furthermore, the copper removal efficiency as high as ~63%, corresponding to removal capacity ≈ 185 mg g^{-1}, was obtained at pH ≈ 4. This removal capacity corresponds to a complete neutralization of the ENCC carboxyl groups by Cu^{2+} ions. Such a high copper uptake at this pH places ENCC among adsorbents with high copper removal capacity.

ASSOCIATED CONTENT

Supporting Information

Snapshots of aggregation and sedimentation of ENCC particles in the presence of 500 ppm of Cu(II) ions; effect of Brownian motion on ENCC aggregate size at different copper concentrations. The Supporting Information is available free of charge on the ACS Publications website at DOI: 10.1021/acsami.5b01619.

AUTHOR INFORMATION

Corresponding Author

*Phone: 514-398-6177. E-mail: theo.vandeven@mcgill.ca.

Author Contributions

‖Amir Sheikhi and Salman Safari contributed equally to this work.

Notes

The authors declare no competing financial interest.

ACKNOWLEDGMENTS

Financial support from an Industrial Research Chair funded by FPInnovations and NSERC and from the NSERC Innovative Green Wood Fibre Products Network are gratefully acknowledged.

REFERENCES

(1) Babel, S.; Kurniawan, T. A. Low-cost Adsorbents for Heavy Metals Uptake from Contaminated Water: a Review. *J. Hazard. Mater.* **2003**, *97*, 219−243.

(2) Panday, K. K.; Prasad, G.; Singh, V. N. Copper(II) Removal from Aqueous Solutions by Fly Ash. *Water Res.* **1985**, *19*, 869−873.

(3) Hua, M.; Zhang, S.; Pan, B.; Zhang, W.; Lv, L.; Zhang, Q. Heavy Metal Removal from Water/Wastewater by Nanosized Metal Oxides: a Review. *J. Hazard. Mater.* **2012**, *211−212*, 317−331.

(4) Mohan, D.; Pittman, C. U. Arsenic Removal from Water/Wastewater Using Adsorbents-a Critical Review. *J. Hazard. Mater.* **2007**, *142*, 1−53.

(5) Nguyen, T. A. H.; Ngo, H. H.; Guo, W. S.; Zhang, J.; Liang, S.; Yue, Q. Y.; Li, Q.; Nguyen, T. V. Applicability of Agricultural Waste and By-products for Adsorptive Removal of Heavy Metals from Wastewater. *Bioresour. Technol.* **2013**, *148*, 574−585.

(6) Demirbas, A. Heavy Metal Adsorption onto Agro-based Waste Materials: a Review. *J. Hazard. Mater.* **2008**, *157*, 220−229.

(7) Suzuki, Y.; Kametani, T.; Maruyama, T. Removal of Heavy Metals from Aqueous Solution by Nonliving Ulva Seaweed as Biosorbent. *Water Res.* **2005**, *39*, 1803−1808.

DOI: 10.1021/acsami.5b01619
ACS Appl. Mater. Interfaces 2015, 7, 11301−11308

(8) Monier, M.; Nawar, N.; Abdel-Latif, D. A. Preparation and Characterization of Chelating Fibers Based on Natural Wool for Removal of Hg(II), Cu(II) and Co(II) Metal Ions from Aqueous Solutions. *J. Hazard. Mater.* **2010**, *184*, 118−125.
(9) Sud, D.; Mahajan, G.; Kaur, M. P. Agricultural Waste Material as Potential Adsorbent for Sequestering Heavy Metal Ions from Aqueous Solutions-a Review. *Bioresour. Technol.* **2008**, *99*, 6017−6027.
(10) Farooq, U.; Kozinski, J. A.; Khan, M. A.; Athar, M. Biosorption of Heavy Metal Ions Using Wheat Based Biosorbents-a Review of the Recent Literature. *Bioresour. Technol.* **2010**, *101*, 5043−5053.
(11) Wu, F.; Tseng, R.; Juang, R. A Review and Experimental Verification of Using Chitosan and Its Derivatives as Adsorbents for Selected Heavy Metals. *J. Environ. Manage.* **2010**, *91*, 798−806.
(12) Li, J.; Zhang, S.; Chen, C.; Zhao, G.; Yang, X.; Li, J.; Wang, X. Removal of Cu(II) and Fulvic Acid by Graphene Oxide Nanosheets Decorated with Fe_3O_4 Nanoparticles. *ACS Appl. Mater. Interfaces* **2012**, *4*, 4991−5000.
(13) Cao, C.; Qu, J.; Wei, F.; Liu, H.; Song, W. Superb Adsorption Capacity and Mechanism of Flowerlike Magnesium Oxide Nanostructures for Lead and Cadmium Ions. *ACS Appl. Mater. Interfaces* **2012**, *4*, 4283−4287.
(14) Chang, Y.; Chen, D. Preparation and Adsorption Properties of Monodisperse Chitosan-bound Fe_3O_4 Magnetic Nanoparticles for Removal of Cu(II) Ions. *J. Colloid Interface Sci.* **2005**, *283*, 446−451.
(15) Gong, J.; Liu, T.; Wang, X.; Hu, X.; Zhang, L. Efficient Removal of Heavy Metal Ions from Aqueous Systems with the Assembly of Anisotropic Layered Double Hydroxide Nanocrystals@Carbon Nanosphere. *Environ. Sci. Technol.* **2011**, *45*, 6181−6187.
(16) Song, J.; Kong, H.; Jang, J. Adsorption of Heavy Metal Ions from Aqueous Solution by Polyrhodanine-encapsulated Magnetic Nanoparticles. *J. Colloid Interface Sci.* **2011**, *359*, 505−511.
(17) Ge, F.; Li, M.; Ye, H.; Zhao, B. Effective Removal of Heavy Metal Ions Cd^{2+}, Zn^{2+}, Pb^{2+}, Cu^{2+} from Aqueous Solution by Polymer-modified Magnetic Nanoparticles. *J. Hazard. Mater.* **2012**, *211−212*, 366−372.
(18) Farrukh, A.; Akram, A.; Ghaffar, A.; Hanif, S.; Hamid, A.; Duran, H. Design of Polymer-brush-grafted Magnetic Nanoparticles for Highly Efficient Water Remediation. *ACS Appl. Mater. Interfaces* **2013**, *5*, 3784−3793.
(19) Paria, S.; Khilar, K. C. A Review on Experimental Studies of Surfactant Adsorption at the Hydrophilic Solidwater Interface. *Adv. Colloid Interface Sci.* **2004**, *110*, 75−95.
(20) Tan, L.; Zhu, D.; Zhou, W.; Mi, W.; Ma, L.; He, H. Preferring Cellulose of Eichhornia Crassipes to Prepare Xanthogenate to Other Plant Materials and Its Adsorption Properties on Copper. *Bioresour. Technol.* **2008**, *99*, 4460−4466.
(21) O'Connell, D. W.; Birkinshaw, C.; O'Dwyer, T. F. Heavy Metal Adsorbents Prepared from the Modification of Cellulose: a Review. *Bioresour. Technol.* **2008**, *99*, 6709−6724.
(22) Belhalfaoui, B.; Aziz, A.; Elandaloussi, E. H.; Ouali, M. S.; Menroval, L. C. D. Succinate-bonded Cellulose: a Regenerable and Powerful Sorbent for Cadmium-removal from Spiked High-hardness Groundwater. *J. Hazard. Mater.* **2009**, *169*, 831−837.
(23) Chen, S.; Zou, Y.; Yan, Z.; Shen, W.; Shi, S.; Zhang, X.; Wang, H. Carboxymethylated-bacterial Cellulose for Copper and Lead Ion Removal. *J. Hazard. Mater.* **2009**, *161*, 1355−1359.
(24) Yu, X.; Tong, S.; Ge, M.; Wu, L.; Zuo, J.; Cao, C.; Song, W. Adsorption of Heavy Metal Ions from Aqueous Solution by Carboxylated Cellulose Nanocrystals. *J. Environ. Sci.* **2013**, *25*, 933−943.
(25) Suopajarvi, T.; Liimatainen, H.; Hormi, O.; Niinimaki, J. Coagulation-flocculation Treatment of Municipal Wastewater Based on Anionized Nanocelluloses. *Chem. Eng. J.* **2013**, *231*, 59−67.
(26) Hokkanen, S.; Repo, E.; Suopajarvi, T.; Liimatainen, H.; Niinimaa, J.; Sillanpaa, M. Adsorption of Ni(II), Cu(II) and Cd(II) from Aqueous Solutions by Amino Modified Nanostructured Microfibrillated Cellulose. *Cellulose* **2013**, *21*, 1471−1487.
(27) Zheng, Q.; Cai, Z.; Gong, S. Green Synthesis of Polyvinyl Alcohol (PVA)-Cellulose Nanofibril (CNF) Hybrid Aerogels and Their Use as Superabsorbents. *J. Mater. Chem. A* **2014**, *2*, 3110−3118.
(28) Klemm, D.; Kramer, F.; Moritz, S.; Lindstrom, T.; Ankerfors, M.; Gray, D.; Dorris, A. anocelluloses: A New Family of Nature-based Materials. *Angew. Chem., Int. Ed.* **2011**, *50*, 5438−5466.
(29) Lin, N.; Dufresne, A. Nanocellulose in Biomedicine: Current Status and Future Prospect. *Eur. Polym. J.* **2014**, *50*, 302−325.
(30) Yang, H.; Tejado, A.; Alam, N.; Antal, M.; Van De Ven, T. Films Prepared from Electrosterically Stabilized Nanocrystalline Cellulose. *Langmuir* **2012**, *28*, 7834−7842.
(31) Safari, S.; Sheikhi, A.; van de Ven, T. Electroacoustic Characterization of Conventional and Electrosterically Stabilized Nanocrystalline Celluloses. *J. Colloid Interface Sci.* **2014**, *432*, 151−157.
(32) Yang, H.; Alam, M.; van de Ven, T. Highly Charged Nanocrystalline Cellulose and Dicarboxylated Cellulose from Periodate and Chlorite Oxidized Cellulose Fibers. *Cellulose* **2013**, 1−11.
(33) Gregory, J. Monitoring Particle Aggregation Processes. *Adv. Colloid Interface Sci.* **2009**, *147−148*, 109−123.
(34) Cuppett, J. D.; Duncan, S. E.; Dietrich, A. Evaluation of Copper Speciation and Water Quality Factors That Affect Aqueous Copper Tasting Response. *Chem. Senses* **2006**, *31*, 689−697.
(35) *PDA Operating Manual. PDA2000 Photometric Dispersion Analyser Operating Manual*; Rank Brothers Ltd.: 2013.
(36) Gaudreault, R.; Cesare, N. D.; Weitz, D.; van de Ven, T. G. M. Flocculation Kinetics of Precipitated Calcium Carbonate. *Colloids Surf., A* **2009**, *340*, 56−65.
(37) Borges, F.; Guimaraes, C.; Lima, J. L. F. C.; Pinto, I.; Reis, S. Potentiometric Studies on the Complexation of Copper(II) by Phenolic Acids as Discrete Ligand Models of Humic Substances. *Talanta* **2005**, *66*, 670−673.
(38) Jeon, C.; Yoo, Y. J.; Hoell, W. H. Environmental Effects and Desorption Characteristics on Heavy Metal Removal Using Carboxylated Alginic Acid. *Bioresour. Technol.* **2005**, *96*, 15−19.
(39) Maekawa, E.; Koshijima, T. Properties of 2,3-Dicarboxy Cellulose Combined with Various Metallic Ions. *J. Appl. Polym. Sci.* **1984**, *29*, 2289−2297.
(40) Hasan, S.; Ghosh, T. K.; Viswanath, D. S.; Boddu, V. M. Dispersion of Chitosan on Perlite for Enhancement of Copper(II) Adsorption Capacity. *J. Hazard. Mater.* **2008**, *152*, 826−837.
(41) Kalyani, S.; Priya, J.; Rao, P.; Krishnaiah, A. Removal of Copper and Nickel from Aqueous Solutions Using Chitosan Coated on Perlite as Biosorbent. *Sep. Sci. Technol.* **2005**, *40*, 1483−1495.
(42) Amarasinghe, B.; Williams, R. Tea Waste as a Low Cost Adsorbent for the Removal of Cu and Pb from Wastewater. *Chem. Eng. J.* **2007**, *132*, 299−309.
(43) Qi, B.; Aldrich, C. Biosorption of Heavy Metals from Aqueous Solutions with Tobacco Dust. *Bioresour. Technol.* **2008**, *99*, 5595−5601.
(44) Wong, K.; Lee, C.; Low, K.; Haron, M. Removal of Cu and Pb from Electroplating Wastewater Using Tartaric Acid Modified Rice Husk. *Process Biochem.* **2003**, *39*, 437−445.
(45) Chakravarty, S.; Pimple, S.; Chaturvedi, H. T.; Singh, S.; Gupta, K. Removal of Copper from Aqueous Solution Using Newspaper Pulp as an Adsorbent. *J. Hazard. Mater.* **2008**, *159*, 396−403.
(46) Aksu, Z.; Isoglu, I. A. Removal of Copper(II) Ions from Aqueous Solution by Biosorption onto Agricultural Waste Sugar Beet Pulp. *Process Biochem.* **2005**, *40*, 3031−3044.
(47) Sun, X.; Peng, B.; Ji, Y.; Chen, J.; Li, D. Chitosan(chitin)/Cellulose Composite Biosorbents Prepared Using Ionic Liquid for Heavy Metal Ions Adsorption. *AIChE J.* **2009**, *55*, 2062−2069.
(48) Low, K.; Lee, C.; Leo, A. Removal of Metals from Electroplating Wastes Using Banana Pith. *Bioresour. Technol.* **1995**, *51*, 227−231.
(49) Basci, N.; Kocadagistan, E.; Kocadagistan, B. Biosorption of copper aiia from aqueous solutions by wheat shell. *Desalination* **2004**, *164*, 135−140.
(50) Sciban, M.; Klasnja, M.; Skrbic, B. Modified Hardwood Sawdust as Adsorbent of Heavy Metal Ions from Water. *Wood Sci. Technol.* **2006**, *40*, 217−227.
(51) Li, N.; Bai, R. Copper Adsorption on Chitosan-cellulose Hydrogel Beads: Behaviors and Mechanisms. *Sep. Purif. Technol.* **2005**, *42*, 237−247.

DOI: 10.1021/acsami.5b01619
ACS Appl. Mater. Interfaces 2015, 7, 11301−11308

(52) Chu, K. H.; Hashim, M. A. Adsorption of Copper(II) and EDTA-chelated Copper(II) onto Granular Activated Carbons. *J. Chem. Technol. Biotechnol.* **2000**, *75*, 1054−1060.
(53) Zhang, G.; Qu, R.; Sun, C.; Ji, C.; Chen, H.; Wang, C.; Niu, Y. Adsorption for Metal Ions of Chitosan Coated Cotton Fiber. *J. Appl. Polym. Sci.* **2008**, *110*, 2321−2327.

DOI: 10.1021/acsami.5b01619
ACS Appl. Mater. Interfaces 2015, 7, 11301−11308